TRENDS IN SCIENCES 2025; 22(8): 10130
https://doi.org/10.48048/tis.2025.10130 RESEARCH ARTICLE

Exploring the Therapeutic Potential of *Leea Indica* Leaf Extract in Diabetic Mice: *In Vivo*, Phytochemical Analysis, and Molecular Interaction Studies

Widhya Aligita[1], Dania Saputri[1], Risma Mariska[1], Putri Regina[2], Rika Kusumawati[2], Ellin Febrina[3] and Aiyi Asnawi[2,*]

[1]*Department of Pharmacology and Clinical Pharmacy, Faculty of Pharmacy, Universitas Bhakti Kencana, Bandung 40617, Indonesia*
[2]*Department of Pharmacochemistry, Faculty of Pharmacy, Universitas Bhakti Kencana, Bandung 40617, Indonesia*
[3]*Department of Pharmacology and Clinical Pharmacy, Faculty of Pharmacy, Universitas Padjadjaran, Jatinangor 45363, Indonesia*

([*]Corresponding author's e-mail: aiyi.asnawi@bku.ac.id)

Received: 9 March 2025, Revised: 24 March 2025, Accepted: 1 April 2025, Published: 20 June 2025

Abstract

Diabetes mellitus remains a global health challenge, with limited effective treatments that address its root causes, including insulin resistance and insulin deficiency. The increasing prevalence of diabetes has required the exploration of alternative treatments, particularly from natural sources. *Leea indica*, a plant known for its medicinal properties, has gained attention for its potential antidiabetic effects. However, there is limited research exploring its therapeutic potential through comprehensive *in vivo*, phytochemical, and molecular docking studies. This study aimed to evaluate the antidiabetic effects of *Leea indica* leaf extract in a model of diabetic mice and explore its molecular mechanisms through docking studies. *In vivo*, results demonstrated that *Leea indica* extract significantly reduced insulin resistance and improved blood glucose regulation in a dose-dependent manner, with the 100 mg dose being particularly effective in lowering glucose levels to near-normal ranges. Histopathological analysis showed that the extract offered protective effects on pancreatic tissue, especially at moderate doses. Furthermore, molecular docking studies revealed that *Leea indica* ligands, NL and S18, exhibited stronger binding affinities for PPAR alpha compared to Acarbose, with the ligand S18 showing a particularly favorable ΔG of −10.6 kcal/mol and Ki of 0.01703 μM. These findings highlight the therapeutic potential of *Leea indica* leaf extract as a promising agent for the treatment of diabetes, with its phytochemicals showing favorable interactions at the molecular level. More research is needed to optimize the dose and understand the mechanisms of action that underlie its antidiabetic effects.

Keywords: *Leea indica*, Phytochemical profile, Molecular docking, Insulin deficiency, Insulin sensitivity

Introduction

Diabetes mellitus is a chronic metabolic disorder that has become a major global health problem and affects millions of people around the world [1]. It is characterized by persistent high blood glucose levels, either due to insulin resistance, insulin deficiency, or a combination of both. Type 1 and type 2 diabetes are the most common forms, with type 2 diabetes being more prevalent [2]. Type 2 diabetes is primarily driven by insulin resistance, where body cells become less responsive to insulin, the hormone responsible for the regulation of blood glucose. As the disease progresses, the pancreas may not produce enough insulin, leading to insulin deficiency. The complexity of diabetes and its related complications, such as cardiovascular disease, neuropathy, and kidney damage, makes it a critical area of medical research.

Although conventional pharmacological treatments, such as insulin therapy and oral

hypoglycemic agents such as metformin, are widely used, they often have side effects and are not always effective in long-term disease management [3]. In addition, the increasing global burden of diabetes highlights the urgent need for alternative, safe, and effective therapeutic options. Herbal remedies, due to their low cost, accessibility, and lower risk of adverse effects, have gained significant attention as potential adjuncts or alternatives to conventional treatments for the management of diabetes [4-6]. Among these, *Leea indica*, a plant native to tropical regions, has shown promise in traditional medicine for its antidiabetic properties, although scientific evidence supporting its efficacy remains limited.

Leea indica, commonly known as "Leea", has been used in various forms to treat a wide range of ailments, including diabetes, inflammation, and digestive problems [7]. Despite its long history of traditional use, there is a gap in research on its therapeutic potential in the management of diabetes using modern scientific methods. Although some studies have suggested that *Leea indica* could have beneficial effects on blood glucose levels and insulin resistance, comprehensive research exploring its mechanisms, effective doses, and overall efficacy is lacking. This research gap motivates the need for more in-depth studies that combine *in vivo*, phytochemical, and molecular docking analyses to fully understand the therapeutic potential of the plant in the treatment of diabetes.

Insulin resistance is a key factor in the development of type 2 diabetes [8,9]. It occurs when body cells, particularly muscle and fat cells, become less responsive to insulin, altering glucose uptake, and leading to elevated blood sugar levels [10]. Over time, this increased demand for insulin can cause pancreatic β-cells to become exhausted and eventually fail, leading to insulin deficiency [11]. Insulin deficiency further exacerbates hyperglycemia, creating a vicious cycle that is difficult to break [12]. Progression from insulin resistance to full-blown diabetes is associated with significant alterations in pancreatic tissue, which can show signs of inflammation, oxidative stress, and β-cell damage [13]. Therefore, any therapeutic agent that can address both insulin resistance and insulin deficiency is critical in the fight against diabetes.

Histopathological examination of pancreatic tissue is an essential tool for evaluating the effects of possible antidiabetic treatments [4]. Damage to pancreatic β-cells, the primary source of insulin production, can be observed in diabetic models, often manifesting as atrophy, inflammation, and fibrosis of the islets [14]. Successful antidiabetic therapy should not only help regulate blood glucose levels but also promote restoration of pancreatic function. Preliminary histological studies suggest that *Leea indica* may have protective effects on pancreatic tissue, reducing damage caused by hyperglycemia and improving insulin secretion. These findings hint at the potential of the plant as a therapeutic agent capable of reversing or slowing the progression of diabetes.

Molecular docking studies provide a powerful computational approach to understanding the interactions between a ligand and its target protein at the molecular level [15,16]. This technique allows researchers to predict the binding affinity of various compounds, offering insight into their potential effectiveness as drug candidates. In the case of *Leea indica*, molecular docking can help identify which bioactive compounds in the extract interact with key proteins involved in glucose metabolism, such as PPAR-α, a nuclear receptor that plays a crucial role in the regulation of insulin sensitivity [17]. By simulating these interactions, it is possible to assess the potential of *Leea indica* phytochemicals to bind to these targets, providing a scientific basis for their antidiabetic effects.

The primary objective of this study was to explore the therapeutic potential of *Leea indica* leaf extract in the management of diabetes, focusing on its effects on insulin resistance, insulin deficiency, and pancreatic health. *In vivo*, studies will evaluate its impact on glucose regulation and insulin sensitivity in a streptozotocin-induced diabetic mouse model. In addition, a detailed phytochemical analysis will be performed to identify the key compounds responsible for its antidiabetic effects. To complement the *in vivo* findings, molecular docking studies will be used to investigate the interactions of *Leea indica* phytochemicals with important molecular targets involved in the pathogenesis of diabetes. By combining these approaches, the study aims to provide a comprehensive understanding of the potential of *Leea indica* as a therapeutic agent.

Materials and methods

Plant determination results

The *Leea indica* plant was subjected to a botanical identification process to confirm its taxonomic classification and ensure its suitability as a research material. This determination was carried out at the Laboratory of Biology of the Faculty of Mathematics and Natural Sciences, Universitas Padjadjaran (FMIPA UNPAD), with the official identification report issued under the number No.28/HB/04/2024. The plant was successfully identified and confirmed as *Leea indica*, which provided the basis for its use in subsequent antidiabetic activity tests.

Ethical committee approval

Before conducting experiments with animals, ethical approval was sought to ensure that the research adhered to appropriate animal welfare standards. The animal ethics approval process was carried out at Universitas Padjadjaran, and the research received formal approval under the ethical permit number No.675/UN6.KEP/EC/2024. This approval ensured that the study met the ethical guidelines for the use of animals in research and that the welfare of the test animals was protected throughout the study.

Preparation of *Leea indica* leaf extract

Leea indica leaves, sourced from Kalangan Gemolong in Sragen, Central Java, Indonesia (coordinates: −7.377735418872041, 110.85746300298734), were collected for the preparation of the extract. A total of 2.5 kg of fresh leaves were thoroughly washed and dried. The dried leaves were then ground using a blender and macerated with 96 % ethanol at room temperature for 24 h. Subsequently, the filtrate was concentrated using a rotary vacuum evaporator.

Phytochemical screening

The phytochemical screening of *Leea indica* leaf extract was carried out to identify the presence of key compounds [18]. To begin, flavonoids were tested using a few drops of a dilute sodium hydroxide solution, which resulted in a yellow coloration, which confirmed the presence of flavonoids. The tannins were then detected by adding a few drops of 1 % ferric chloride solution, which produced a dark blue-black color, indicating the presence of tannins. For saponins, the extract was mixed with water and stirred vigorously; the formation of a stable foam confirmed the presence of saponins.

The alkaloids were identified by adding a few drops of Dragendorff's reagent to the extract, which produced an orange precipitate, suggesting the presence of alkaloids. Lastly, the extract was tested for steroids and terpenoids by reacting it with Liebermann-Burchard reagent, which resulted in a greenish-blue color, confirming the presence of these compounds. This screening showed that *Leea indica* leaf extract contained a variety of bioactive compounds, including flavonoids, tannins, saponins, alkaloids, and steroids/terpenoids.

Insulin resistance animal model

In this study, the animal subjects used were 2 - 3 month-old male Balb-C mice, weighing between 20 - 30 g, and in healthy condition (non-diabetic). A total of 30 mice were randomly divided into 6 groups, with 5 mice in each group. The mice were acclimatized for 7 days to ensure that they adapted to the new environment and minimized potential stress from environmental changes. During the acclimatization period, they received normal food and had free access to drinking water. The Insulin Resistance Animal Model was conducted preventively by orally administering a 20 % lipomed MCT/LCT (20 % lipid emulsion) induction solution at a dose of 10 mL/kg of body weight, along with oral treatment for 21 days, to prevent induction-induced blood glucose increase [4].

After acclimatization, mice were fasted for 3 h before measuring their baseline blood glucose levels. The mice were then divided into 6 groups: Negative control (Na CMC 0.5 %), positive control (induction only), a standard drug group (metformin 65 mg/kg of body weight), and 3 treatment groups that received ethanol extracts of *Leea indica* leaves at doses of 50, 100 and 200 mg/kg of body weight [19]. Following the baseline measurement of blood glucose, treatments were administered according to the assigned group. On day 21, after fasting for 3 h, insulin tolerance was assessed by administering insulin at a dose of 0.1 U / kg of body weight by intraperitoneal injection. Blood glucose levels were measured every 15 for 60 min using the Easy Touch® blood glucose test meter. The main parameter observed was the constant insulin tolerance test (KTTI).

Insulin-Deficiency animal model

In this study, the test animals used were Balb-C strain mice, aged 2 - 3 months, weighing between 20 - 30 g and in healthy condition (non-diabetic). A total of 30 mice were randomly divided into 6 groups, with 5 mice in each group. After an adaptation period, all groups, except Group I (normal), were induced with streptozotocin (STZ) at a dose of 35 mg/kg of body weight. 3 days after induction, blood glucose levels were measured in all mice. On the same day, treatment interventions were administered according to the following schedule. The normal control group received only standard feed, the standard drug group received glibenclamide at 0.013 mg/kg of body weight, and the positive control group was treated with 0.5 % carboxymethylcellulose (CMC).

All remaining groups were induced with STZ to induce diabetes but received varying doses of *Leea indica* leaf ethanolic extract. The third group, Dose I, received a lower dose of the extract at 50 mg/kg of body weight. The 4 group, Dose II, received a higher dose of 100 mg/kg of body weight, while the fifth group, Dose III, received the highest dose of 200 mg/kg of body weight. The treatment was conducted for 21 days.

Blood glucose levels were measured at three-time points: On day 3 after induction (to evaluate the initial effect of STZ), and again on days 7, 14, and 21 to evaluate the ongoing impact of treatments on the diabetic condition. This study aimed to assess the potential of *Leea indica* leaf extract to manage blood glucose levels in diabetic mice.

Histopathological examination

Histological examination of the pancreas of mice treated with *Leea indica* leaf extract was performed using hematoxylin and eosin (H&E) staining. This technique was used to color the tissue and highlight structural details. Hematoxylin stained the cell nuclei blue, allowing for clear visualization of the cell's core structures, while eosin stained the cytoplasm red, providing a contrasting color to the nuclei. The stained pancreatic tissue was then observed under a microscope at 400× magnification, allowing the evaluation of any histopathological changes caused by the treatment of *Leea indica* leaf extract. This method helped evaluate the impact of the extract on the pancreas at the cellular level.

LC-MS/MS analysis

The procedure for LC-MS/MS analysis of phytochemicals in *Leea indica* leaf extract was conducted following a detailed protocol. Initially, 10.00 mg of *Leea indica* leaf extract was carefully weighed and dissolved in methanol within a 10 mL measuring flask. The extract solution was mixed thoroughly to ensure complete dissolution. From this solution, 5 µL was taken using a micro syringe and injected into the sample location of the LC-MS/MS system for analysis.

High-resolution mass spectrometry experiments were performed using an ultra-performance liquid chromatography (UPLC) system (ACQUITY UPLC® H-Class System, Waters, USA) coupled with a mass spectrometer (Xevo G2-S QTof, Waters, USA). A C18 column (1.8 µm, 2.1×100 mm, ACQUITY UPLC® HSS, Waters, USA) was used for the separation of phytochemicals. The column temperature was maintained at 50 °C, while the room temperature was set at 25 °C to ensure optimal separation conditions.

For LC analysis, a mobile phase consisting of water with 5 mM ammonium formate (A) and acetonitrile with 0.05 % formic acid (B) was used. The mobile phase was run at a flow rate of 0.2 mL/min in a step gradient over 23 min to achieve an effective separation of the compounds. Before injection, the sample solution was filtered through a 0.2 µm syringe filter to remove any particulates and 5 µL of the filtered solution was injected into the system.

Mass spectrometry (MS) analysis was performed using electrospray ionization (ESI) in positive mode, which allowed the detection of positively charged ions. The mass spectrometer was set to scan a mass range of 50 to 1,200 m/z, covering the expected molecular weights of the phytochemicals in the extract. The source and desolvation temperatures were optimized to ensure effective ionization of the compounds and minimal sample loss.

The separation results were then processed by the QToF-MS detector, which produced chromatogram peaks corresponding to the individual phytochemicals in the *Leea indica* leaf extract. These chromatogram peaks were subsequently interpreted using MassLynx software, allowing the identification of the phytochemicals based on their mass-to-charge (m/z) ratios and retention times.

Molecular docking simulation

The molecular docking simulation of phytochemicals from *Leea indica* leaf extract to enzymes responsible for insulin production (PPAR alpha with PDB ID 1I7I) and insulin sensitivity (insulin tyrosine kinase with PDB ID 1IR3) followed a structured procedure. [5,20,21] First, the 3D structures of the phytochemicals that adhered to Lipinski's rules were obtained by downloading the corresponding structure data files (*.sdf) from the PubChem database. These structures were then subjected to geometric optimization using the Avogadro application [22], resulting in the output files being saved in *.pdb format, ready for docking simulations.

Next, the 3D structures of the target enzymes: PPAR alpha (PDB ID 1I7I) and insulin tyrosine kinase (PDB ID 1IR3) were prepared by downloading their respective crystal structures from the Protein Data Bank (www.rcsb.org). Any heteroatoms, water molecules, or cocrystallized ligands were removed to ensure a clean docking environment. The proteins were then preprocessed and saved in a format compatible with the AutoDock 4.2 software for further molecular docking simulations.

Before the phytochemicals, a validation of the docking procedure was carried out. This involved redocking the native ligands of PPAR alpha (PDB ID 1I7I) and insulin tyrosine kinase (PDB ID 1IR3) back into their respective active sites. The validation was deemed successful by ensuring that the root mean square deviation (RMSD) between the re-docked pose and the original ligand conformation was within acceptable limits (< 2 Å), thereby confirming the precision of the docking parameters and the dimensions of the grid box.

Following validation, the optimized phytochemicals of *Leea indica* leaf extract were docked into the active sites of PPAR alpha and insulin tyrosine kinase using AutoDock 4.2 [23]. The docking simulations were performed in an automated manner, where the binding energies and molecular interactions were calculated based on the optimal docking positions of each phytochemical at the enzyme's binding site. Grid box dimensions and docking parameters were selected based on the validated docking procedure to ensure consistency.

Finally, the molecular interactions of phytochemicals with enzymes were analyzed using the Discovery Studio Visualizer 2021 application. This software provided detailed information on the binding energy and binding modes of the phytochemicals. The results included information on hydrogen bonding, hydrophobic interactions, and other key molecular interactions between the phytochemicals and the active site residues of the enzymes, which were then used to assess the potential of the phytochemicals as modulators of insulin production and sensitivity.

Molecular dynamics simulation

The molecular dynamics (MD) simulations were conducted using GROMACS 2023, with the primary goal of investigating the interactions of the ligands with the receptor protein [16,24]. The simulations were carried out on a high-performance computing system equipped with an Intel Xeon E5-2690v3 processor, 32 GB of RAM, and an NVIDIA RTX 3070 GPU, which provided the necessary computational power for running the 100 ns simulations efficiently.

The first step in the simulation process involved preparing the system, which included generating the topology files for the protein-ligand complex. The topologies were created using ACPYPE (A Python-based tool for generating force field parameters) [25], which allowed the ligands to be properly parameterized and compatible with the GROMACS force fields. Two of the best-performing ligands from the molecular docking simulations were selected for further analysis in the molecular dynamics simulations. These ligands were then docked into the receptor's binding site, and the resulting protein-ligand complexes were prepared for the MD simulation. The system was solvated in a cubic box of water molecules, and sodium or chloride ions were added to neutralize the charge of the system. Energy minimization was performed to remove any steric clashes and to relax the system before the actual molecular dynamics simulations were initiated. The production MD runs were performed for 100 ns, allowing the system to equilibrate and reach a stable conformation, providing valuable insights into the dynamic behavior and stability of the protein-ligand interactions.

Results and discussion

Phytochemical screening

The results of the phytochemical screening of *Leea indica* leaf extract revealed the presence of several bioactive compounds, each of which contributed to the potential therapeutic properties of the plant. Alkaloids were detected in the extract. Alkaloids are known for their wide range of biological activities, including anti-inflammatory, analgesic, and antidiabetic effects [24,26,27]. Their presence suggests that *Leea indica* could help alleviate some of the inflammatory symptoms associated with diabetes and potentially offer pain relief for diabetic patients.

Flavonoids were also identified in the extract, indicating their significant presence. Flavonoids are well known for their antioxidant properties and have been shown to improve insulin sensitivity and protect against oxidative stress, two key factors involved in the development and progression of diabetes [28]. This suggests that the flavonoids in *Leea indica* may help prevent the oxidative damage that is often seen in diabetics.

Quinones, another class of compounds, were also found. Quinones are organic compounds with antimicrobial and antioxidant properties, which could contribute to reducing oxidative stress and protecting against infections, a common complication of diabetes [29]. Saponins were also present and are known for their ability to lower blood sugar levels, improve lipid metabolism, and enhance immune function, making them highly beneficial for the management of diabetes [30].

Tannins were also detected in the extract, contributing to its anti-inflammatory, antimicrobial, and antioxidant properties [31,32]. These properties are particularly important in reducing complications such as infections and tissue damage, which are common in diabetic patients. Lastly, triterpenoids were identified. These compounds are recognized for their anti-inflammatory, antihyperglycemic, and antioxidant activities, which may support their role in the management of diabetic conditions [33].

In conclusion, the phytochemical evaluation of *Leea indica* leaf extract highlighted the presence of a variety of bioactive compounds, including alkaloids, flavonoids, quinones, saponins, tannins, and triterpenoids. These compounds are well known for their potential to combat oxidative stress, inflammation, and metabolic dysfunctions associated with diabetes. These findings support the hypothesis that *Leea indica* may have significant antidiabetic activity, probably due to the synergistic effects of these phytochemicals. More research is needed to fully understand the specific mechanisms by which these compounds work to manage diabetes and its complications.

Insulin resistance

The insulin resistance animal model is a widely used method to evaluate the effects of various treatments on glucose metabolism and insulin sensitivity [34]. In this study, the model was applied to mice to assess changes in insulin resistance by measuring the constant insulin tolerance test (CTTI). CTTI values, measured at baseline (T0) and after 21 days of treatment (T21), provide information on the insulin response of the animals and the effectiveness of different therapeutic interventions. Average values of the insulin tolerance test constant (KTTI) in the animal model at two-time points: T0 (pre-treatment) and T21 (after 21 days of treatment) (**Table 1**). The KTTI values reflect the ability of the mice to respond to insulin, providing insight into the development of insulin resistance and the effectiveness of different treatments.

From the data presented in (**Table 1**), it can be observed that the Normal Control group had an initial CTTI value of 3.63 ± 0.83 at T0, which increased significantly to 7.66 ± 1.66 at T21 ($^{*}p < 0.05$). This increase suggests that the normal control group developed a noticeable degree of insulin resistance during 21 days, probably due to the induction process used in the model.

The positive control group, which received induction alone, also showed a significant increase in KTTI, from 3.55 ± 1.35 at T0 to 7.23 ± 2.02 at T21 ($^{*}p < 0.05$). This increase indicates that induction alone was effective in creating insulin resistance in mice. However, the standard drug group (metformin) did not show a significant change in KTTI (2.91 ± 1.04 in T0 to 2.93 ± 1.49 in T21, $^{\#@}p < 0.05$). The minimal change in CTTI in this group suggests that metformin effectively maintained the insulin sensitivity of mice, preventing the progression of insulin resistance.

In the treatment groups (Dose I, Dose II, and Dose III), CTTI values also increased with time, reflecting the

progression of insulin resistance. For Dose I, CTTI increased from 3.36 ± 1.07 in T0 to 6.87 ± 4.76 in T21 ($^{*}p < 0.05$), while Dose II and Dose III showed similar trends, with significant increases in CTTI from 3.38 ± 1.74 to 7.00 ± 2.40 ($^{*}p < 0.05$) and from 3.40 ± 1.03 to 7.17 ± 3.35 ($^{*}p < 0.05$), respectively. These results suggest that the treatments provided some level of protection against the development of insulin resistance, although their effects were less potent than metformin, as indicated by the comparison with the Positive Control and Metformin groups.

Table 1 Average KTTI values in the animal model at T0 and T21 ($n = 6$).

Group	T0 (pretreatment)	T21 (Day 21)
Normal Control	3.63 ± 0.83	7.66 ± 1.66*
Standard drug (Metformin, 65 mg/gram BW)	2.91 ± 1.04	2.93 ± 1.49$^{\#@}$
Positive Control	3.55 ± 1.35	7.23 ± 2.02*
Dose I (treatment group 1)	3.36 ± 1.07	6.87 ± 4.76*
Dose II (treatment group 2)	3.38 ± 1.74	7.00 ± 2.40*
Dose III (treatment group 3)	3.40 ± 1.03	7.17 ± 3.35*

$^{\#}(p < 0.05)$: Indicates a significant difference compared to the positive control group.
$^{*}(p < 0.05)$: Indicates a significant difference compared to the negative control group.
$^{@}(p < 0.05)$: Indicates a significant difference compared to the Metformin group.

In general, the data from this study demonstrate that insulin resistance was successfully induced in the animal model and that the treatments had varying levels of effectiveness in preventing or mitigating insulin resistance. Metformin was the most effective in maintaining insulin sensitivity, while the other treatments, although beneficial, did not perform as well compared to them. These findings emphasize the importance of testing different compounds in insulin resistance models to evaluate their potential as therapeutic agents for diabetes and metabolic disorders.

Insulin deficiency

The study investigated the effects of *Leea indica* leaf extract on blood glucose levels in streptozotocin-induced diabetic mice over a 21-day treatment period. The results, shown in (**Table 2**), revealed varying responses between the treatment groups compared to the normal control and positive control groups. On day 0, blood glucose levels were similar in all groups, with the normal control group at 86.8 ± 9.73 mg/dL, and other groups showed comparable levels. On day 7, significant changes were observed. The standard drug group saw a marked increase in blood glucose to 291 ± 16.92 mg/dL, significantly higher than the normal control and positive control groups. This marked elevation continued through days 14 and 21, with blood glucose levels increasing to 293 ± 14.23 and 296 ± 16.36 mg/dL, respectively.

Table 2 Average blood glucose levels from day 0 to day 21 of treatment ($n = 6$).

Group	T0 (Day 0)	T7 (Day 7)	T14 (Day 14)	T21 (Day 21)
Normal Control	86.8 ± 9.73	89.2 ± 6.26$^{\#}$	86.8 ± 4.08$^{\#}$	88.8 ± 3.96$^{\#}$
Standard Drug	85.6 ± 9.56	291 ± 16.92$^{*\wedge}$	293 ± 14.23$^{*\wedge}$	296 ± 16.36$^{*\wedge}$
Positive Control	85 ± 9.02	92 ± 8$^{\#}$	88.2 ± 7.98$^{\#}$	91.6 ± 4.03$^{\#}$
Dose I	90.6 ± 10.31	181.4 ± 7.86$^{*\#\wedge}$	151.6 ± 13.44$^{*\#\wedge}$	127.6 ± 3.64$^{*\#\wedge}$
Dose II	84.2 ± 3.42	166.6 ± 14.77$^{*\#\wedge}$	130.2 ± 7.66$^{*\#\wedge}$	97.8 ± 9.09$^{\#}$
Dose III	97.4 ± 5.89	113.8 ± 10.63$^{*\#\wedge}$	95.2 ± 4.91$^{\#}$	90.2 ± 6.30$^{\#}$

(*) Indicates a significant difference compared to the normal control group.
(#) Indicates a significant difference compared to the Positive Control group.
(^) Indicates a significant difference compared to the Comparison Group.

On the contrary, the groups receiving *Leea indica* leaf extract (Dose I, II, and III) showed a more favorable response. Blood glucose levels in Dose I decreased significantly from 181.4 ± 7.86 mg/dL on day 7 to 127.6 ± 3.64 mg/dL on day 21, suggesting a potential beneficial effect on glucose metabolism. Dose II also showed a decrease, from 166.6 ± 14.77 mg/dL on day 7 to 97.8 ± 9.09 mg/dL on day 21. This decrease in blood glucose levels was statistically significant compared to the normal control and positive control groups.

The most notable improvement was observed in Dose III, where blood glucose levels decreased from 113.8 ± 10.63 mg/dL on day 7 to 90.2 ± 6.30 mg/dL on day 21. These results were significantly different from those of both the positive control and the comparison groups, indicating that the highest dose of *Leea indica* extract had a positive impact on the reduction of elevated blood glucose levels [4].

The normal control and positive control groups exhibited stable blood glucose levels throughout the study, with the normal control group maintaining levels around 86 - 89 mg/dL and the positive control group showing slight fluctuations (92 ± 8 on day 7, 88.2 ± 7.98 on day 14 and 91.6 ± 4.03 on day 21). However, the standard drug group consistently had much higher glucose levels, suggesting that the streptozotocin-induced diabetic state was not adequately controlled by the standard drug in this experiment.

In conclusion, *Leea indica* leaf extract demonstrated a significant reduction in blood glucose levels in diabetic mice, particularly at higher doses, indicating its potential as a therapeutic agent for the management of diabetes. These results suggest that *Leea indica* could be a promising natural treatment for controlling blood glucose levels under diabetic conditions.

Histopathological examination

In this study, histological observations were made in pancreatic cells and tissues of mice following different treatments. The results revealed notable differences in the island area, cell count, and cell density between the experimental groups, suggesting various levels of tissue response to *Leea indica* leaf extract and the standard drug, glibenclamide. The Normal Control Group showed the largest island area, with a value of 30.115 μm², and the highest cell density at 371 cells/μm². This group had the healthiest pancreatic tissue, with well-preserved cells and normal tissue architecture, indicating stable pancreatic function and no signs of diabetic-induced damage. The Standard Drug Group (Glibenclamide), which received glibenclamide, showed a significantly smaller island area (15.008 μm²) compared to the normal group [35]. Despite this reduction, the cell density increased to 428 cells/μm², suggesting that glibenclamide could have promoted cell proliferation or reduced cell death in pancreatic tissue, improving the overall condition of the pancreas in diabetic mice.

The Positive Control Group (which was not treated after being induced with diabetes) exhibited a sharp decrease in both the island area (9.172 μm²) and the cell density (271 cells/μm²), indicating severe damage to the pancreatic islets due to sustained hyperglycemia [36]. The pancreas of this group showed atrophy and reduced cell counts, consistent with the progression of diabetes in untreated mice. On the contrary, the groups treated with varying doses of *Leea indica* leaf extract showed a range of effects on pancreatic tissue, the Dose I group (50 mg of extract) showing a moderate island area (14,210.77 μm²) and a cell density of 319 cells/μm². Although the island area was smaller than in the normal group, this suggests that *Leea indica* extract may help preserve pancreatic islet structure, even at a lower dose.

The Dose II group (100 mg of extract) showed an island area of 15.889 μm² and a cell count of 72 cells, with a lower cell density of 222 cells/μm². This could indicate that while the extract helps preserve the islet area, it can also reduce cell density, potentially due to a lesser regenerative effect compared to glibenclamide. On the other hand, the Dose III Group (200 mg of extract) showed the highest island area at 33.734 μm² and the highest cell count at 152, although with the lowest cell density at 218 cells/μm². This suggests that the higher dose of *Leea indica* may have stimulated cell proliferation, leading to a larger islet size, but the density of the cells was somewhat reduced, which may reflect the complex balance of regeneration and cell expansion [37].

In general, the histological results indicated that *Leea indica* leaf extract, especially at higher doses,

showed the potential to preserve the morphology of the pancreatic islet and promote cellular changes, although the effects varied by dose. While glibenclamide improved cell density and helped maintain islet structure, the effects of the extract were dose-dependent, with positive and less favorable results observed at different doses. More research is needed to better understand the mechanisms by which *Leea indica* affects pancreatic tissue, particularly in terms of cell regeneration and islet preservation in diabetic conditions.

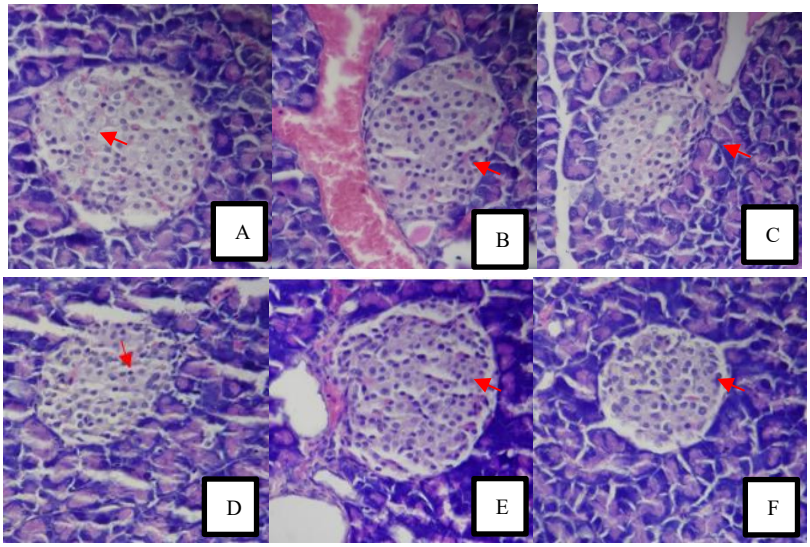

Figure 1 Histological analysis of cells and tissues in mice.

Phytochemical profile

The phytochemical profile of *Leea indica* leaf extract was analyzed using LC-MS/MS, and retention times and fragmentation patterns were interpreted to identify several compounds [38]. According to the chromatogram in (**Figure 2**), various phytochemicals were detected in a wide range of retention times, from compounds eluting early at 1.70 min to those eluting as late as 17.73 min. Interpretation of these retention times, combined with MS/MS fragmentation data presented in (**Table 3**), allowed the identification of a diverse set of molecules, indicating the complexity of the phytochemical composition of the *Leea indica* leaf extract.

At a retention time of 1.70 min, the compound identified was 2-(dimethylamino) acetohydrazide ($C_4H_{12}N_3O$), a small nitrogen-containing compound with a molecular weight of 118.0937 m/z. This early eluting compound suggests its relatively polar nature, which is consistent with the presence of hydrazide and amino groups, making it a hydrophilic molecule. Its identification adds to the understanding of nitrogenous compounds present in the extract.

As the retention time increased, more complex molecules were detected. For example, at 5.08 min, a compound with a mass of 420.1881 m/z was identified as 20-(2,5-Dioxo-2,5-dihydro-1H-pyrrol-1-yl)-3,6,9,12,15,18-hexaoxaicosan-1-oic acid ($C_{18}H_{30}NO_{10}$), which is a much larger and likely more lipophilic molecule compared to compounds eluting earlier. Its structure suggests the presence of multiple ether linkages, indicating potential bioactivity since such structures are often involved in biological transport or membrane interaction processes.

The presence of flavonoids in the *Leea indica* extract was confirmed at retention times of 5.58 and 6.15 min, where luteolin ($C_{15}H_{11}O_6$) was identified with an m/z value of 287.0557 and 287.0526, respectively. This compound is a well-known flavonoid with antioxidant properties, and its identification in the extract aligns with previous reports on the bioactive compounds found in *Leea indica*. The detection of luteolin at 2 close retention times suggests either the presence of isomers or differences in ionization states during the analysis.

One of the more complex compounds identified at 11.07 min was Boldenone Undecylenate ($C_{30}H_{45}O_3$), with a molecular weight of 453.3377 m/z. Boldenone is

a steroidal compound and its identification in *Leea indica* leaf extract may suggest that the plant contains bioactive components with potential hormonal or anabolic activities, although its role in the plant's biological profile remains to be further studied.

A significant portion of the detected compounds remained unidentified. For example, at 6.44 min, a compound with a mass of 482.2606 m/z and the molecular formula $C_{17}H_{36}N_7O_9$ was observed but not identified. The presence of several unknown compounds with high molecular weights, such as those detected at retention times of 13.51 min (496.3421 m/z) and 15.89 min (824.5532 m/z), suggests that *Leea indica* leaf extract contains novel or less studied bioactive molecules that warrant further investigation.

The identification of known and unknown compounds in the chromatographic profile highlights the chemical diversity of *Leea indica* leaf extract. The presence of flavonoids such as luteolin, along with more complex nitrogenous and steroidal compounds, indicates the potential pharmacological significance of the plant. Further exploration of unknown compounds could uncover new phytochemicals with unique biological activities.

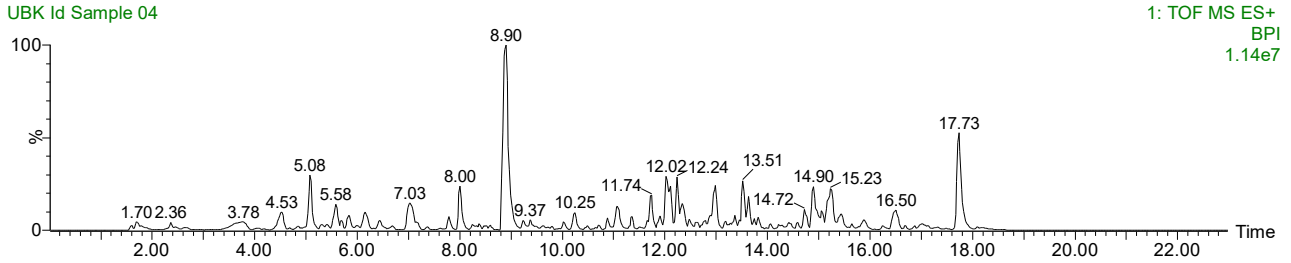

Figure 2 TICs of the chromatogram and the phytochemical peaks of the *Leea indica* leaf extract. 70 % ethanol was used as the extraction solvent.

Table 3 Phytochemical compounds identified from *Leea Indica* leaf extract by HPLC-Q-TOF-MS.

Entry	Retention time (min)	MS/MS fragment ions (m/z)	Molecular formula	Identified phytochemical
S01	1.70	118.0937	$C_4H_{12}N_3O$	2-(Dimethylamino)acetohydrazide
S02	2.36	136.0712	$C_3H_{10}N_3O_3$	1,3,5-Triazinane-1,3,5-triol
S03	3.78	120.0814	$C_8H_{10}N$	Indoline
S04	4.53	188.0714	$C_7H_6N_7$	6-(1H-Imidazol-1-yl)tetrazolo[1,5-b]pyridazine
S05	5.08	420.1881	$C_{18}H_{30}NO_{10}$	20-(2,5-Dioxo-2,5-dihydro-1H-pyrrol-1-yl)-3,6,9,12,15,18-hexaoxaicosan-1-oic acid
S06	5.58	287.0557	$C_{15}H_{11}O_6$	Luteolin
	6.44	482.2606	$C_{17}H_{36}N_7O_9$	Unknown
S07	7.03	197.1180	$C_{11}H_{17}O_3$	1-carboxy-3-hydroxyadamantane
S08	7.78	301.0718	$C_{12}H_9N_6O_4$	4,6-Di(1H-1,2,4-triazol-1-yl)isophthalic acid
S09	8.00	331.0826	$C_{13}H_{11}N_6O_5$	N-(1,3-Benzodioxol-5-yl)-5-(1-methyl-4-nitro-1H-imidazol-5-yl)-1,3,4-oxadiazol-2-amine
S10	8.38	225.1130	$C_8H_{13}N_6O_2$	A-134U
S11	8.90	315.0870	$C_{13}H_{11}N_6O_4$	N-(1H-Benzotriazol-1-ylmethyl)-3,5-dinitroaniline
	9.37	656.4362	$C_{27}H_{54}N_{13}O_6$	N~6~-(N~6~-Carbamimidoyl-L-lysyl)-N-{(2S)-4-amino-1-
S12	10.25	297.1400	$C_{21}H_{17}N_2$	Lophine

Entry	Retention time (min)	MS/MS fragment ions (m/z)	Molecular formula	Identified phytochemical
S13	11.07	453.3377	$C_{30}H_{45}O_3$	Boldenone Undecylenate
S14	11.74	636.4104	$C_{35}H_{58}NO_9$	(2S,3Z,5S,6S,7S,8Z,11S,12R,13S,14S,15S,16Z)-14-(Carbamoyloxy)-6,12-dihydroxy-1-[(2S,3R,4S,5R)-4-hydroxy-3,5-dimethyl-6-oxotetrahydro-2H-pyran-2-yl]-5,7,9,11,13,15-hexamethyl-3,8,16,18-nonadecatetraen- 2-yl acetat
S15	12.02	638.4260	$C_{31}H_{56}N_7O_7$	L-Prolyl-L-lysyl-L-prolyl-L-leucyl-L-alanyl-L-leucine
S16	12.24	518.3254	$C_{22}H_{44}N_7O_7$	asp-lys-lys-lys
	12.33	638.4241	$C_{31}H_{56}N_7O_7$	L-Prolyl-L-lysyl-L-prolyl-L-leucyl-L-alanyl-L-leucine
S17	12.99	353.2700	$C_{17}H_{33}N_6O_2$	5-[4-(2-Ethoxyethyl)-1-piperazinyl]-4-methyl-N-(3-pentanyl)-4H-1,2,4-triazole-3-carboxamide
	13.51	496.3421	$C_{20}H_{46}N_7O_7$	Unknown
S18	13.63	445.3683	$C_{25}H_{45}N_6O$	4-[(Cyclohexylmethyl)amino]-N-isobutyl-2-{[3-(2-methyl-1-piperidinyl)propyl]amino}-5-pyrimidinecarboxamide
	13.82	522.3563	$C_{19}H_{40}N_{17}O$	Unknown
S19	14.59	443.3891	$C_{26}H_{47}N_6$	(4S)-1-(4-{(4S)-3-[2-(Adamantan-1-yl)ethyl]-2-imino-4-imidazolidinyl}butyl)-4-butyl-2-imidazolidinimine
	14.72	700.4468	$C_{29}H_{62}N_7O_{12}$	Unknown
	14.90	524.3718	$C_{18}H_{46}N_{13}O_5$	Unknown
	15.23	622.4307	$C_{31}H_{56}N_7O_6$	Unknown
	15.45	622.4307	$C_{31}H_{56}N_7O_6$	Unknown
	15.89	824.5532	$C_{41}H_{74}N_7O_{10}$	Unknown
S20	16.50	611.4669	$C_{39}H_{63}O_5$	(2S)-3-Hydroxy-2-[(9Z,12Z,15Z)-9,12,15-octadecatrienoyloxy]propyl (6Z,9Z,12Z,15Z)-6,9,12,15-octadecatetraenoate
	17.73	954.6239	$C_{46}H_{84}N_9O_{12}$	Unknown

Molecular interaction

The docking procedure for the identified phytochemicals from *Leea indica* leaf extract was validated by docking the natural ligands of the target enzymes, PPAR alpha (PDB ID 1I7I) [39] and insulin tyrosine kinase (PDB ID 1IR3) [40], using AutoDock 4.2 software. This validation step was crucial for ensuring the reliability of the docking protocol before proceeding with the docking of the identified phytochemicals to these enzymes. Redocking of the native ligands to the active sites of the enzymes helped determine how well the docking method reproduced the known binding poses and interactions. The validation process focused on key parameters such as the root mean square deviation (RMSD), the binding energy, and the inhibition constant (Ki) [16,41].

The validation of the docking procedure for PPAR alpha with PDB ID 1I7I resulted in an RMSD of 1.080 Å, which indicated good agreement between the re-docked ligand and the experimental ligand structure

(**Figure 3(a)**). Typically, RMSD values below 2 Å were considered acceptable for accurate docking predictions, showing that the procedure successfully reproduced the binding pose. The binding energy obtained was −9.43 kcal/mol, suggesting a strong interaction between the ligand and the active site of PPAR alpha. The inhibition constant (Ki) was calculated to be 122.39 nM, reflecting a powerful inhibitory effect on the enzyme, which is consistent with the known role of PPAR alpha in the regulation of insulin production.

For the insulin tyrosine kinase (PDB ID 1IR3), the docking procedure validation produced an RMSD of 1.586 Å (**Figure 3(b)**). Although slightly higher than that for the PPAR alpha validation, this value was still within the acceptable range, indicating that the docking method could adequately predict the binding mode of the native ligand. The binding energy for insulin tyrosine kinase was found to be −7.05 kcal / mol, suggesting a moderate interaction between the ligand and the enzyme's active site. The inhibition constant was calculated to be 6.83 μM, indicating a lower inhibitory effect compared to PPAR alpha, consistent with the role of insulin tyrosine kinase in insulin sensitivity rather than direct insulin production.

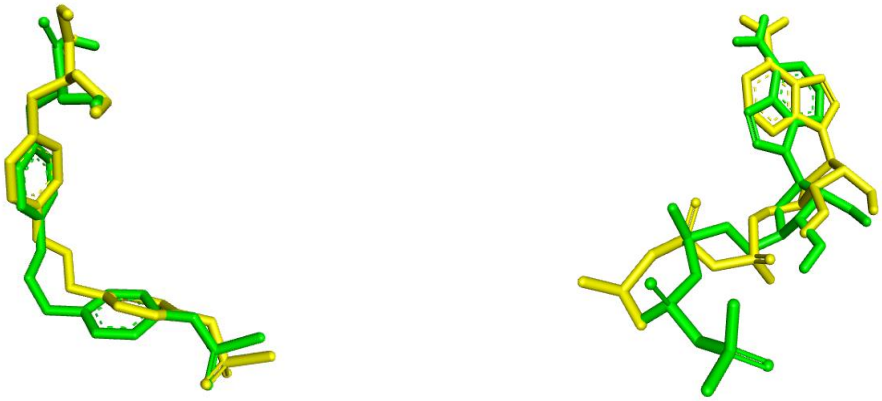

(a) (b)

Figure 3 Overlay visualization of the native ligand from redocking results (yellow) and X-ray crystallography (green) at the binding sites of PPAR alpha (PDB ID 1I7I) (a) and insulin tyrosine kinase (PDB ID 1IR3) (b).

The grid parameters used during the docking procedure were optimized to capture the active sites of the enzymes effectively. For both PPAR alpha and insulin tyrosine kinase, the grid box was set to 56×50×56 points^3 with a grid spacing of 0.375 Å. The center of the grid for PPAR alpha was located at X = 21.677, Y = 23.38, and Z = 13.884, while for insulin tyrosine kinase, it was established at X = −26.556, Y = 30.12, and Z = 7.546. These grid settings ensured that the ligands were accurately placed in the active sites, enabling precise interaction analysis.

In conclusion, validation of the docking procedure demonstrated that AutoDock 4.2 successfully reproduced native ligand binding poses for both PPAR alpha and insulin tyrosine kinase. The satisfactory RMSD values and binding energies indicated that the docking protocol was reliable for further investigation of the interaction between the identified phytochemicals of *Leea indica* and these enzymes. This validation step provided confidence in the pairing results to explore the potential of these phytochemicals to modulate insulin production and sensitivity.

Binding energy

The validated docking procedure was then applied to docking the identified phytochemicals of *Leea indica* to the active sites of PPAR alpha and insulin tyrosine kinase. This step was crucial in predicting the possible binding interactions of compounds such as luteolin, boldenone undecylenate, and other nitrogenous compounds identified in the LC-MS/MS analysis (**Table 4**). Since the docking parameters had been validated through re-docking, the predicted binding energies and inhibition constants for these

phytochemicals could be considered reliable indicators of their potential activity against these enzymes involved in insulin regulation.

The molecular docking simulations for the identified phytochemicals of *Leea indica* leaf extract were performed using a validated docking procedure to evaluate their binding energies to 2 enzymes, PPAR alpha (PDB ID 1I7I) and insulin tyrosine kinase (PDB ID 1IR3), which are key regulators of insulin production and sensitivity. The docking simulations were limited to phytochemicals that adhered to Lipinski's rules for drug-likeness, ensuring their potential as oral therapeutic agents [42]. The binding energy (ΔG) and inhibition constant (Ki) values of these compounds were compared to a native ligand (NL) and acarbose, a standard drug used for the treatment of diabetes.

Table 4 Binding Energy and Inhibition Constant of *Leea Indica* Leaf Phytochemicals at Binding Sites of PPAR Alpha (PDB ID 1I7I) and Insulin Tyrosine Kinase (PDB ID 1IR3).

Entry	PDB ID 1I7I		PDB ID 1IR3	
	ΔG (kcal/mol)	Ki (uM)	ΔG (kcal/mol)	Ki (uM)
NL	−9.43	0.12239	−7.05	6.83
S01	−4.28	727.87	−5.02	208.26
S02	−4.14	919.91	−4.03	1,120
S03	−5.26	139.72	−4.98	222.83
S04	−6.6	14.43	−6.17	29.84
S06	−7.44	3.51	−7.57	2.85
S07	−6.42	19.65	−4.59	434.04
S08	−5.82	54.18	−4.28	733.24
S09	−9.15	0.19618	−6.86	9.3
S10	−4.99	221.52	−5.33	124.9
S11	−8.59	0.50723	−7.53	3.01
S17	−7.56	2.87	−6.05	36.58
S18	−10.6	0.01703	−8.02	1.33
Acarbose	−5.27	137.3	−4.87	268.33

For PPAR alpha (PDB ID 1I7I), the phytochemicals exhibited a wide range of binding affinities, with S18 showing the strongest interaction, having a binding energy of −10.6 kcal/mol and an inhibition constant of 0.01703 μM. This was significantly lower than the binding energy of the native ligand of −9.43 kcal/mol, indicating a stronger binding affinity. S09 and S11 also showed high binding affinities with energies of −9.15 and −8.59 kcal/mol, respectively, and low Ki values, suggesting that they could be promising candidates for modulating insulin production. On the contrary, phytochemicals such as S01 and S02 had much weaker binding energies, with ΔG values of −4.28 and −4.14 kcal/mol, indicating relatively poor interactions with PPAR alpha.

Similarly, for insulin tyrosine kinase (PDB ID 1IR3), S18 again demonstrated the strongest binding affinity with a ΔG value of −8.02 kcal/mol and a Ki of 1.33 μM, outperforming the binding energy of the native ligand of −7.05 kcal/mol. This was closely followed by S06 and S11, which exhibited binding energies of −7.57 and −7.53 kcal/mol, respectively, suggesting potential roles in improving insulin sensitivity. In contrast, weaker interactions were observed for compounds such as S01 and S02, with ΔG values of −5.02 and −4.03 kcal/mol, respectively, indicating a lower likelihood of effectively modulating insulin sensitivity.

Compared to acarbose, which had a binding energy of −5.27 kcal/mol for PPAR alpha and −4.87 kcal/mol for insulin tyrosine kinase, several *Leea indica* phytochemicals demonstrated superior binding affinities. In particular, S18, S09, and S11 consistently outperformed acarbose in both enzyme targets, suggesting that these compounds might possess stronger antidiabetic properties than the standard drug. This comparison highlighted the potential of *Leea indica* phytochemicals as natural alternatives or complements to existing diabetes treatments.

The docking results also revealed that certain compounds exhibited a selective affinity for one enzyme over the other. For example, S09 showed a strong interaction with PPAR alpha (ΔG = −9.15 kcal/mol) but a moderate binding energy with insulin tyrosine kinase (ΔG = −6.86 kcal/mol). Similarly, S17 had a higher binding affinity for PPAR alpha (−7.56 kcal/mol) than for insulin tyrosine kinase (−6.05 kcal/mol). These findings suggest that some phytochemicals may preferentially target insulin production rather than insulin sensitivity, or vice versa.

In general, molecular docking simulations provided valuable insight into the binding affinities of *Leea indica* phytochemicals to key enzymes involved in insulin regulation. Several compounds, particularly S18, S09, and S11, demonstrated strong binding energies that exceeded both native ligands and acarbose, positioning them as promising candidates for further investigation as potential antidiabetic agents. The results supported the notion that *Leea indica* leaf extract contains bioactive compounds with potential therapeutic applications in the management of diabetes.

Binding mode

Binding interactions of 4-[(Cyclohexylmethyl) amino] -N-isobutyl-2- [3- (2-methyl-1-piperidinyl) propyl] amino-5-pyrimidinecarboxamide (S18) with enzymes responsible for insulin production (PPAR alpha, PDB ID 1I7I) and insulin sensitivity (insulin tyrosine kinase, PDB ID 1IR3) revealed significant molecular interactions (**Figure 4**). For PPAR alpha, S18 established four hydrogen bonds (HB) with the amino acid residues Arg74, Ile75, Glys78, and Cys79. These hydrogen bonds are crucial for stabilizing the complex and contribute to the binding affinity of the compound. Furthermore, S18 formed five hydrophobic interactions (HI) with residues Ile135, Leu124, Met158, Arg82, and Lys59, further enhancing its binding within the active site of PPAR alpha.

The combination of hydrogen bonding and hydrophobic interactions for S18 with PPAR alpha resulted in a strong binding energy of −9.43 kcal/mol, indicating a stable interaction. The calculated inhibition constant (Ki) of 122.39 nM suggests a high binding affinity, which means that S18 may effectively modulate the activity of PPAR alpha, potentially influencing insulin production. The interactions between S18 and the hydrophobic residues within the binding pocket, particularly with residues such as Met158 and Ile135, indicate a well-fitted binding mode that maximized the interaction of the compound with the enzyme.

For insulin tyrosine kinase (PDB ID 1IR3), S18 formed three hydrogen bonds with the residues Ser29, Asp173, and Gly172. These hydrogen bonds provided stability to the complex but were fewer in number compared to the interactions with PPAR alpha. Despite this, the presence of eight hydrophobic interactions with the residues Val33, Leu25, Ala51, Met176, Met162, Val83, Met102, and Met99 compensated for the fewer hydrogen bonds. The extensive hydrophobic interactions indicated that S18 fits well into the hydrophobic regions of the insulin tyrosine kinase binding pocket, likely contributing to its binding stability.

The binding energy of S18 with insulin tyrosine kinase was measured at −7.05 kcal/mol, slightly less than its interaction with PPAR alpha, but still indicating a favorable interaction. The inhibition constant for this complex was calculated to be 6.83 μM, which is higher compared to the value for PPAR alpha, suggesting a lower binding affinity to insulin tyrosine kinase. This difference in binding affinity might suggest that S18 has a more prominent effect on insulin production than on insulin sensitivity, as reflected in its stronger interaction with PPAR alpha.

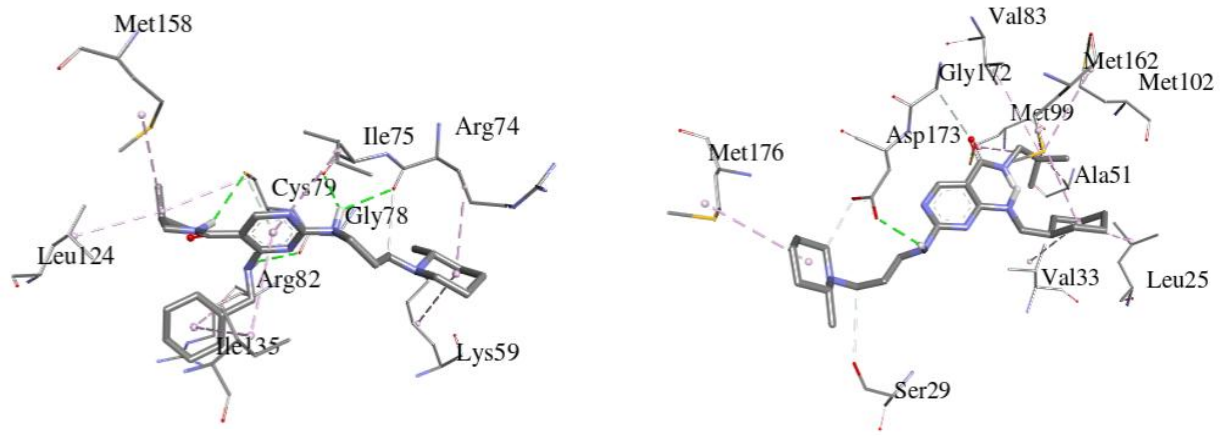

(a) (b)

Figure 4 3D visualization of S18 (4- [(Cyclohexylmethyl) amino] -N-isobutyl-2- [3- (2-methyl-1-piperidinyl)propyl] amino -5-pyrimidinecarboxamide) at the binding sites of PPAR alpha (PDB ID 1I7I) (a) and Insulin tyrosine kinase (PDB ID 1IR3) (b).

In general, S18 demonstrated a potent interaction with PPAR alpha and insulin tyrosine kinase through hydrogen bonding and hydrophobic interactions. However, the stronger binding affinity to PPAR alpha highlights its potential role in modulating insulin production more effectively than insulin sensitivity. The molecular interactions observed in this study suggest that S18 could be a promising candidate for further development as an antidiabetic compound, particularly in the targeting of insulin production pathways.

Stability of the complex from MD simulations

The RMSD analysis of AZ2, S18, and S09 in complex with PDB ID 1I7I, carried out over a 100 ns molecular dynamics simulation using Gromacs 2023, revealed distinct behaviors for each ligand (**Figure 5(a)**). For AZ2, the RMSD fluctuated moderately throughout the simulation, with an initial value of 0.0004699 nm at time 0 ns, gradually increasing to around 0.2759 nm by 100 ns. This indicates that AZ2, being the native ligand, maintains a stable but slightly variable interaction with the receptor over time, reflecting a balanced binding affinity. S18 showed a higher degree of fluctuation compared to AZ2, starting at 0.0005049 nm and rising to 0.3009 nm by the end of the simulation. The RMSD values for S18 suggest a less stable binding to the protein, with noticeable deviations that could indicate potential conformational changes or weaker interactions.

On the other hand, S09 exhibited the highest level of fluctuation, with its RMSD increasing from 0.0004992 nm at 0 ns to 0.8081 nm at 100 ns. This substantial rise in RMSD suggests that S09 undergoes significant conformational changes and may not bind as stably to the protein as AZ2 or S18. The trend of increasing RMSD for S09 was particularly evident after the first 50 ns, where its values peaked and remained elevated throughout the remainder of the simulation. This behavior indicates that S09 may be less suited for stable binding to the receptor compared to AZ2, further supporting the hypothesis that ligand stability plays a critical role in protein-ligand interactions.

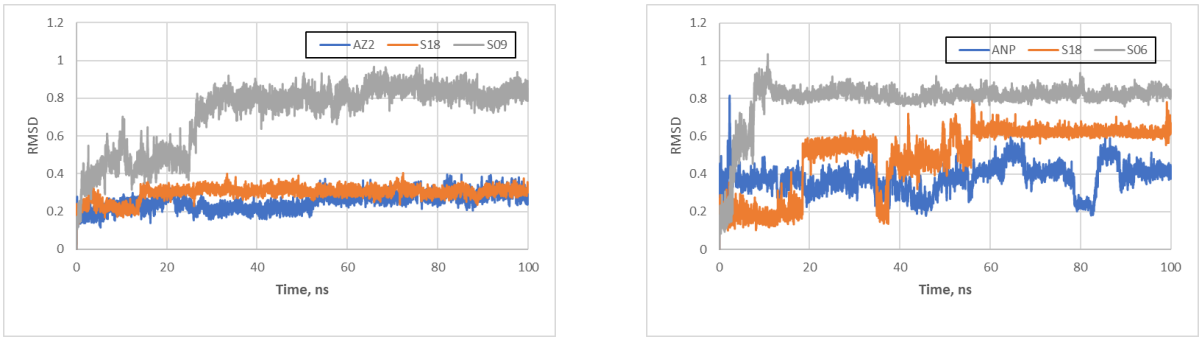

(a) (b)

Figure 5 RMSD of the 100 ns MD simulation complexes for PDB ID 1I7I (a) and PDB ID 1IR3 (b), showing the stability of the protein-ligand complexes over time.

The RMSD analysis of ANP, S18, and S06 in complex with PDB ID 1IR3 over a 100 ns molecular dynamics simulation using Gromacs 2023 revealed different stabilities for each ligand (**Figure 5(b)**). ANP, the native ligand, exhibited relatively stable binding throughout the simulation. It started with a very low RMSD of 0.000505 nm at time 0 ns and showed moderate fluctuations, peaking at around 0.5282 nm at 85 ns, before returning to 0.4387 nm at 100 ns. This suggested that ANP maintained a stable but slightly dynamic interaction with the receptor, reflecting a balance between flexibility and stability during the simulation. In contrast, S18 displayed more significant fluctuations in its RMSD. Initially, its RMSD was 0.0004707 nm, but it rose to 0.6666 nm at 60 ns before settling around 0.6180 nm at 100 ns. These larger fluctuations indicated that S18 interacts with the protein less stably compared to ANP, with potential conformational changes affecting its binding.

S06, similar to S18, showed considerable variations in its RMSD throughout the simulation. Starting with a low RMSD of 0.0004728 nm at 0 ns, it reached a peak of 0.8838 nm at 80 ns before settling at 0.8102 nm at 100 ns. These larger deviations in RMSD indicated that S06 undergoes significant conformational changes and may have a less stable binding to the protein compared to ANP. While S06 was able to form an initial interaction with the receptor, its binding was less stable over the 100 ns period, as suggested by the sharp increase in RMSD around 80 ns. Overall, the analysis highlighted that ANP remained the most stable ligand, while both S18 and S06 displayed more dynamic behaviors, with S06 showing the greatest instability in its interaction with the receptor.

Energy components

The energy component analysis of AZ2, S18, and S09 in complex with PDB ID 1I7I, performed over a 100 ns molecular dynamics simulation using Gromacs 2023, provided insights into the stability and binding efficiency of each ligand (**Figure 6(a)**). AZ2, the native ligand, exhibited a favorable overall binding energy, with a ΔTOTAL of −38.48 kcal/mol. The decomposition of its energy components showed a significant contribution from the van der Waals interactions (ΔVDWAALS = −52.77 kcal/mol), indicating strong nonbonded interactions with the receptor.[43] However, the electrostatic energy (ΔEEL = −19.86 kcal/mol) was also relatively favorable, while the solvation energy (ΔGSOLV = 34.16 kcal/mol) was somewhat higher, suggesting that the desolvation penalty slightly impacted its stability. Despite this, AZ2's binding remained energetically favorable, reflected in its negative total energy.

In comparison, S18 demonstrated a more substantial total energy contribution (ΔTOTAL = −67.47 kcal/mol), with a particularly strong van der Waals interaction (ΔVDWAALS = −69.76 kcal/mol), indicating a robust physical interaction with the receptor. However, S18's electrostatic energy (ΔEEL = −16.19 kcal/mol) and solvation energy (ΔGSOLV = 18.48 kcal/mol) were less favorable than AZ2's, which could suggest a less optimal balance between favorable interactions and solvation effects. On the other hand, S09 showed a similar pattern of energy components with

a total energy of −37.27 kcal/mol, but its van der Waals interaction (ΔVDWAALS = −43.2 kcal/mol) was weaker compared to AZ2 and S18, indicating a potentially less stable binding mode. The relatively higher solvation energy (ΔGSOLV = 22.03 kcal/mol) for S09 also indicated that it faced a greater desolvation penalty than the other ligands, further reducing its binding stability. This analysis highlighted that while S18 showed the most negative total energy, both AZ2 and S09 had less favorable energy components in some areas, suggesting that S18 had the most stable overall interaction with the receptor.

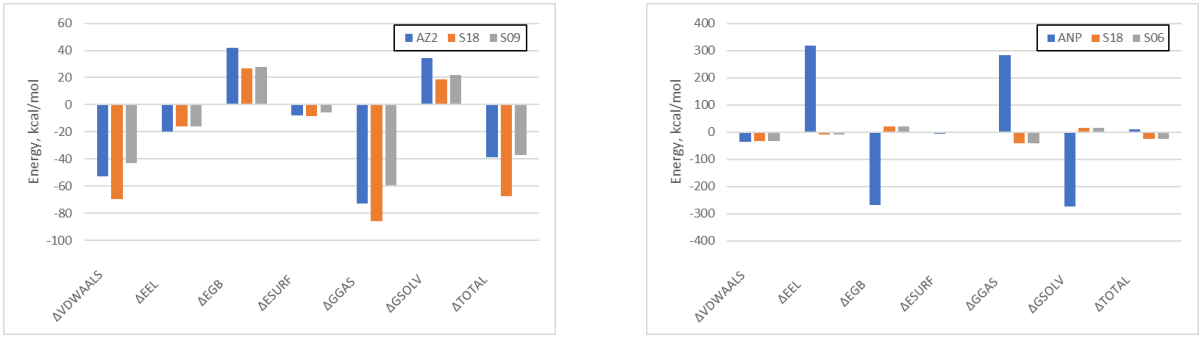

(a) (b)

Figure 6 Energy components of the 100 ns MD simulation complexes for PDB ID 1I7I (a) and PDB ID 1IR3 (b), highlighting the contributions of van der Waals, electrostatic, and solvation energies to the overall binding stability.

The energy component analysis of ANP, S18, and S06 in complex with PDB ID 1IR3 from the 100 ns molecular dynamics simulation using Gromacs 2023 showed distinct differences in the binding energies of each ligand (**Figure 6(b)**). ANP, the native ligand, exhibited a relatively favorable binding energy with a ΔTOTAL of 9.37 kcal/mol, despite the positive value. This was largely due to the favorable van der Waals interactions (ΔVDWAALS = −36.97 kcal/mol) and electrostatic contributions (ΔEEL = 319.3 kcal/mol). However, ANP's large positive electrostatic term was offset by a significant unfavorable contribution from the solvation energy (ΔGSOLV = −272.97 kcal/mol), suggesting that the solvation process played a major role in the ligand's stability. The energy components suggested that while ANP formed strong interactions with the receptor, the overall solvation effects were not optimal, slightly raising the total energy.

In contrast, S18 and S06 exhibited less favorable energy profiles. Both ligands had negative total energies, with S18 having a ΔTOTAL of −25.78 kcal/mol and S06 showing a ΔTOTAL of −26.31 kcal/mol. Despite having favorable van der Waals interactions, with values of −33.48 kcal/mol for S18 and −32.72 kcal/mol for S06, both ligands experienced unfavorable electrostatic interactions, with S18 having a ΔEEL of −7.94 kcal/mol and S06 a similar value of −9.94 kcal/mol. Additionally, both ligands had significant positive electrostatic energies in their solvation components, with ΔEGB values of 20.1 and 21.01 kcal/mol for S18 and S06, respectively. These unfavorable solvation energies (ΔGSOLV = 15.64 kcal/mol for S18 and ΔGSOLV = 16.35 kcal/mol for S06) highlighted that the solvation effects were less optimal for these ligands, contributing to their overall higher total energy compared to ANP. This analysis suggested that, while both S18 and S06 could bind to the protein, their interactions were less stable than ANP's, primarily due to less favorable electrostatic and solvation components.

The comparison between the binding energy from molecular docking and the MMGBSA energy calculated from molecular dynamics simulations revealed interesting differences in the stability and interactions of the ligands (**Table 4** and **Figure 6(a)**). For AZ2, the native ligand of PDB ID 1I7I, the binding energy from molecular docking was −9.43 kcal/mol, while the MMGBSA energy from the 100 ns molecular dynamics simulation was significantly more negative at −38.48 kcal/mol. This large difference suggested that the molecular dynamics simulation, which considers the flexibility of the ligand and receptor over time, provided a more accurate and stable measure of the binding affinity, reflecting a stronger and more consistent

interaction in the dynamic environment. Similarly, for S18, the molecular docking binding energy was −10.6 kcal/mol, but the MMGBSA energy was much more negative at −67.47 kcal/mol, indicating that, once the system dynamics were accounted for, the binding was even more energetically favorable than predicted by docking alone.

For S09, the molecular docking binding energy was −9.15 kcal/mol, and the MMGBSA energy came out to −37.27 kcal/mol, showing a similar trend where the molecular dynamics simulation suggested a stronger overall binding. These results indicated that while molecular docking provided an initial estimate of the binding energy, the MMGBSA calculations from molecular dynamics simulations gave a deeper, more accurate insight into the ligand-receptor interactions. The increased negative values of MMGBSA energies, especially for S18, suggested that including the dynamic behavior of the system over time, such as conformational changes and solvent effects, was crucial for understanding the true binding affinity of the ligands. Overall, this comparison highlighted the importance of using molecular dynamics to refine and validate predictions made by molecular docking, particularly in more complex systems.

The comparison between the binding energies from molecular docking and the MMGBSA energies derived from molecular dynamics simulations for ANP, S18, and S06 revealed notable discrepancies that highlight the importance of accounting for molecular flexibility and environmental factors (**Table 4** and **Figure 6(b)**). For ANP, the native ligand of PDB ID 1IR3, the binding energy from molecular docking was −7.05 kcal/mol, suggesting a moderately favorable interaction with the receptor. However, when considering the MMGBSA energy from the molecular dynamics simulation, the value shifted dramatically to 9.37 kcal/mol. This positive MMGBSA energy indicated that, in the dynamic simulation, the overall interaction became less favorable due to factors such as solvation effects, electrostatic interactions, and receptor-ligand flexibility. The significant difference suggests that the docking model might have overlooked some of the dynamic contributions that impacted the binding stability over time.

Similarly, for S18 and S06, the molecular docking binding energies were −8.02 and −7.57 kcal/mol, respectively, which indicated relatively favorable binding in the static model. However, the MMGBSA results from the molecular dynamics simulations showed much more negative values for both ligands, with S18 at −25.78 kcal/mol and S06 at −26.31 kcal/mol. These more negative MMGBSA energies suggested that, when accounting for the flexibility of the system, both ligands were predicted to bind more stably to the receptor in the dynamic environment. The differences between the docking and MMGBSA results for all three ligands highlighted the importance of molecular dynamics simulations in providing a more realistic and comprehensive view of ligand-receptor interactions. The static docking energies appeared to underestimate the influence of dynamic factors, such as conformational changes and solvation, which were better captured in the MMGBSA calculations.

As a note, this study had several limitations that should be considered. The use of diabetic mice may not have fully reflected human diabetes, and the short duration of the experiment limited the assessment of long-term effects and potential side effects of Leea Indica leaf extract. Additionally, the specific dosages tested may not have applied universally, and the exact bioactive compounds responsible for therapeutic effects were not fully identified. Molecular docking results were based on theoretical models that required further experimental validation, and the small sample size of the animal model reduced the generalizability of the findings. Lastly, environmental factors could have influenced the results, and larger, standardized studies were needed to confirm the outcomes.

Conclusions

This study highlighted the potential of *Leea indica* leaf extract as an effective antidiabetic agent, as it significantly reduces insulin resistance and improves blood glucose regulation in a dose-dependent manner. The extract, especially at a 100 mg dose, was particularly effective in lowering blood glucose to near-normal levels, with promising histopathological evidence suggesting beneficial effects on pancreatic tissue. Furthermore, histopathological analysis suggests that *Leea indica* extract may offer protective benefits to pancreatic tissue, especially in moderate doses. Molecular docking results reveal that the ligands NL and S18 demonstrated a stronger binding affinity compared

to Acarbose, with more favorable ΔG and Ki values, particularly for S18 with ΔG of −10.6 kcal/mol and Ki of 0.01703 μM for PPAR alpha. These findings support further investigation of the therapeutic potential of *Leea indica* for the treatment of diabetes, with a focus on optimizing dosages and exploring its underlying mechanisms. These findings support the potential use of *Leea indica* as a therapeutic agent for diabetes, with further research needed to determine its optimal dosage and mechanisms of action of its phytochemicals.

Acknowledgements

The authors would like to express their sincere gratitude to Bhakti Kencana University, Indonesia for providing access to their laboratory facilities and for supporting this research through the 2024 DRPM Internal Research Grant. We are deeply appreciative of the financial support and the resources provided by Universitas Bhakti Kencana, Indonesia, which were essential to the successful completion of this study.

Declaration of Generative AI in Scientific Writing

The authors acknowledge the use of generative AI tools (e.g., QuillBot and ChatGPT by OpenAI) in the preparation of this manuscript, specifically for language editing and grammar correction. No content generation or data interpretation was performed by AI. The authors take full responsibility for the content and conclusions of this work.

CRediT author statement

Widhya Aligita: Conceptualization, Methodology, Supervision, Validation, Funding acquisition, and Writing – original draft.

Dania Saputri: Data curation, Formal analysis, Investigation, Validation, and Visualization.

Risma Mariska: Data curation, Formal analysis, Investigation, Validation, and Visualization.

Putri Regina: Data curation, Formal analysis, Investigation, Validation, and Visualization.

Rika Kusumawati: Data curation, Formal analysis, Investigation, Validation, and Visualization.

Ellin Febrina: Methodology, Project administration, Resources, Supervision, Validation, and Writing – original draft.

Aiyi Asnawi: Conceptualization, Resources, Software, Funding acquisition, and Writing – review & editing.

References

[1] CDC. *Diabetic ketoacidosis*. CDC, Bangkok, Thailand, 2021.

[2] S Chatterjee, PK Khunti and PMJ Davies. Type 2 diabetes. *The Lancet* 2017; **389(10085)**, 2239-2251.

[3] IH Kuan, RL Savage, SB Duffull, RJ Walker and DF Wright. The association between metformin therapy and lactic acidosis. *Drug Safety* 2019; **42**, 1449-1469.

[4] W Aligita, S Muhsinin, E Susilawati, D Pratiwi, D Aprilliani, A Artarini and I Adnyana. Antidiabetic activity of okra (*Abelmoschus esculentus* L.) fruit extract. *RASAYAN Journal of Chemistry* 2019; **12(1)**, 157-167.

[5] Nursamsiar, Marwati, Khairuddin, FJ Sami, H Kasmawati, W Aligita, E Febrina and A Asnawi. Isolation, characterization, and in vitro inhibitory activity of a new alpha-glucosidase inhibitor from *Schleichera oleosa* (Lour.) *Oken* leaves. *Journal of Pharmacy & Pharmacognosy Research* 2025; **13(1)**, 140-151.

[6] ASV Wyk and G Prinsloo. Health, safety and quality concerns of plant-based traditional medicines and herbal remedies. *South African Journal of Botany* 2020; **133**, 54-62.

[7] F Hossain, MG Mostofa and AK Alam. Traditional uses and pharmacological activities of the genus leea and its phytochemicals: A review. *Heliyon* 2021; **7**, e06222.

[8] NI Ischak, LO Aman, H Hasan, AL Kilo and A Asnawi. *In silico* screening of Andrographis paniculata secondary metabolites as anti-diabetes mellitus through PDE9 inhibition. *Research in Pharmaceutical Sciences* 2023; **18(1)**, 100-111.

[9] YT Wondmkun. Obesity, insulin resistance, and type 2 diabetes: Associations and therapeutic implications. *Diabetes, Metabolic Syndrome and Obesity* 2020; **13**, 3611-3616.

[10] MS Rahman, KS Hossain, S Das, S Kundu, EO Adegoke, MA Rahman, MA Hannan, MJ Uddin and P Myung-Geol. Role of insulin in health and

disease: An update. *International Journal of Molecular Sciences* 2021; **22(12)**, 6403.

[11] M Prentki, P Marie-Line, P Masiello and SRM Madiraju. Nutrient-Induced metabolic stress, adaptation, detoxification, and toxicity in the pancreatic β-Cell. *Diabetes* 2020; **69(3)**, 279-290.

[12] NKZ Zolkeflee, PL Wong, M Maulidiani, NS Ramli, A Azlan and Fh Abas. Metabolic alterations in Streptozotocin–nicotinamide-induced diabetic rats treated with muntingia calabura extract via ^{1}H-NMR-based metabolomics. *Planta Medica* 2023; **89(9)**, 916-934.

[13] PA Gerber and GA Rutter. The role of oxidative stress and hypoxia in pancreatic Beta-Cell dysfunction in diabetes mellitus. *Antioxidants & Redox Signaling* 2017; **26(10)**, 501-518.

[14] DL Eizirik, L Pasquali and M Cnop. Pancreatic β-cells in type 1 and type 2 diabetes mellitus: Different pathways to failure. *Nature Reviews Endocrinology* 2020; **16(7)**, 349-362.

[15] AKA Gunawan, PS Yustiantara, PMNA Sari, DK Wati, MY Putra and IMAG Wirasuta. *In silico* and multivariate analysis of herbal compounds in asthma inflammation: Exploring alternatives to corticosteroids. *Tropical Journal of Natural Product Research* 2025; **9(2)**, 817-825.

[16] E Febrina and A Asnawi. Lead compound discovery using pharmacophore-based models of small-molecule metabolites from human blood as inhibitor cellular entry of SARS-CoV-2. *Journal of Pharmacy & Pharmacognosy Research* 2023; **11(5)**, 810-822.

[17] Y Li, N Ks, G Byran and PT Krishnamurthy. Identification of selective PPAR-γ modulators by combining pharmacophore modeling, molecular docking, and adipogenesis assay. *Applied Biochemistry and Biotechnology* 2023; **195(2)**, 1014-1041.

[18] L Kousalya, P Seethapathy, D Pandita, S Packiaraj, S Venkatesh, S Sankaralingam, M Arunkumar, B Harinathan, A Pandita, R Casini, EA Mahmoud, IM Moussa and HO Elansary. Chitosan (CTS) induced secondary metabolite production in Canscora decussata Schult. - An endangered medicinal plant. *Kuwait Journal of Science* 2025; **52(1)**, 100306.

[19] OE Ayegbusi, OT Aladesanmi, OE Kosemani and OA Adewusi. Effects of lead chloride on growth performance of clarias gariepinus (Burchell, 1822). *International Journal of Bioassays* 2018; **7(5)**, 5638-5644.

[20] LO Aman, NI Ischak, TS Tuloli, A Arfan and A Asnawi. Multiple ligands simultaneous molecular docking and dynamics approach to study the synergetic inhibitory of curcumin analogs on ErbB4 tyrosine phosphorylation. *Research in Pharmaceutical Sciences* 2024; **19(6)**, 754-765.

[21] A Asnawi, E Febrina, W Aligita, LO Aman and F Razi. Molecular docking and molecular dynamics study of 3-hydroxybutyrate with polymers for diabetic ketoacidosis-targeted molecularly imprinted polymers. *Journal of Pharmacy & Pharmacognosy Research* 2024; **12(5)**, 822-836.

[22] HD Snyder and TG Kucukkal. Computational chemistry activities with Avogadro and ORCA. *Journal of Chemical Education* 2021; **98(4)**, 1335-1341.

[23] GM Morris, R Huey, W Lindstrom, MF Sanner, RK Belew, DS Goodsell and AJ Olson. AutoDock4 and AutoDockTools4: Automated docking with selective receptor flexibility. *Journal of Computational Chemistry* 2009; **30(16)**, 2785-2791.

[24] A Asnawi, S Mieldianisa, W Aligita, A Yuliantini and E Febrina. Integrative computational approaches for designing novel alpha-glucosidase inhibitors based on curculigoside A derivatives: Virtual screening, molecular docking, and molecular dynamics. *Journal of Herbmed Pharmacology* 2024; **13(2)**, 308-323.

[25] A Bernardi, R Faller, D Reith and KN Kirschner. ACPYPE update for nonuniform 1–4 scale factors: Conversion of the GLYCAM06 force field from AMBER to GROMACS. *SoftwareX* 2019; **10**, 100241.

[26] I Muhammad, N Rahman, U Nishan and M Shah. Antidiabetic activities of alkaloids isolated from medicinal plants. *Brazilian Journal of Pharmaceutical Sciences* 2021; **57**, e19130.

[27] Nursamsiar, S Nur, E Febrina, A Asnawi and S Syafiie. Synthesis and Inhibitory Activity of Curculigoside A Derivatives as Potential Anti-

Diabetic Agents with β-Cell Apoptosis. *Journal of Molecular Structure* 2022; **1265**,133292

[28] SP Manavi, T Amiri and MJ Mozafaryan. Role of flavonoids in diabetes. *Journal of Reviews in Medical Sciences* 2021; **1(3)**, 149-161.

[29] MAD Junior, RWN Edzang, AL Catto and JM Raimundo. Quinones as an efficient molecular scaffold in the antibacterial/antifungal or antitumoral arsenal. *International Journal of Molecular Sciences* 2022; **23(22)**, 14108.

[30] N Choudhary, GL Khatik and A Suttee. The possible role of saponin in type-II diabetes-a review. *Current diabetes reviews* 2021; **17(2)**, 107-121.

[31] D Kurnia, D Meilinawati, L Marliani, E Febrina and A Asnawi. A review of tannin compounds in avocado as antioxidants. *Tropical Journal of Natural Product Research* 2024; **8(10)**, 8607-8616.

[32] Z Tong, W He, X Fan and A Guo. Biological function of plant tannin and its application in animal health. *Frontiers in Veterinary Science* 2022; **8**, 803657.

[33] Shivam, AK Gupta and S Kumar. Review on diabetic complications and their management by flavonoids and triterpenoids. *The Natural Products Journal* 2023; **13(8)**, 105-114.

[34] SH Lee, SY Park and CS Choi. Insulin resistance: from mechanisms to therapeutic strategies. *Diabetes & Metabolism Journal* 2022; **46(1)**, 15-37.

[35] Z Zeng, L Liang, Z Feng, P Guo, X Hao, J Xian, H Feng, Y Chen and Z Chen. Glibenclamide pretreatment attenuates early hematoma expansion of warfarin-associated intracerebral hemorrhage in rats by alleviating perihematomal blood–brain barrier dysfunction. *Chinese Neurosurgical Journal* 2024; **10(01)**, 8-19.

[36] J Zhang, X Wang, Y Lv, J Hou, C Zhang, X Su and L Li. Impact of stress hyperglycemia on long-term prognosis in acute pancreatitis without diabetes. *Internal and Emergency Medicine* 2024; **19(3)**, 681-688.

[37] B Pucelik, A Barzowska and A Czarna. DYRK1A inhibitors leucettines and TGF-β inhibitor additively stimulate insulin production in beta cells, organoids, and isolated mouse islets. *Plos One* 2023; **18(5)**, e0285208.

[38] AME Sayed, SM Basam, EMBA El-Naggar, HS Marzouk and S El-Hawary. LC–MS/MS and GC–MS profiling as well as the antimicrobial effect of leaves of selected Yucca species introduced to Egypt. *Scientific Reports* 2020; **10(1)**, 17778.

[39] P Cronet, JF Petersen, R Folmer, N Blomberg, K Sjoblom, U Karlsson, EL Lindstedt and K Bamberg. Structure of the PPARα and-γ ligand binding domain in complex with AZ 242; ligand selectivity and agonist activation in the PPAR family. *Structure* 2001; **9(8)**, 699-706.

[40] SR Hubbard. Crystal structure of the activated insulin receptor tyrosine kinase in complex with peptide substrate and ATP analog. *The EMBO Journal* 1997; **16(18)**, 5572-5581.

[41] A Asnawi, LO Aman, Nursamsiar, A Yuliantini and E Febrina. Molecular docking and molecular dynamic studies: screening phytochemicals of *Acalypha indica* against BRAF kinase receptors for potential use in melanocytic tumours. *RASAYAN Journal of Chemistry* 2022; **15(02)**, 1352-1361.

[42] TK Karami, S Hailu, S Feng, R Graham and HJ Gukasyan. Eyes on Lipinski's rule of five: A New "rule of thumb" for physicochemical design space of ophthalmic drugs. *Journal of Ocular Pharmacology and Therapeutics* 2022; **38(1)**, 43-55.

[43] E Febrina, P Regina, Y Susilawati, FF Sofian and A Asnawi. *In silico* screening of *Laminaria japonica* ligands as potential inhibitors of DPP-4 for type 2 diabetes treatment. *Tropical Journal of Natural Product Research* 2025; **9(1)**, 157-167.